



EUS2- Lille, 12-16 December 2022

Search for site specific ion-molecule reactions



SAPIENZA
UNIVERSITÀ DI ROMA

Maria Elisa Crestoni

Dipartimento di Chimica e Tecnologie del Farmaco,
Sapienza Università di Roma, P.le A. Moro 5, I-00185, Roma (Italy)



Ion-Molecule Reactions

- in Multiple-Stage Mass Spectrometers (ion isolation + reactions with specific gaseous reagent under low-energy, controlled conditions)
- High degree of experimental flexibility (different ionization sources)
- IMRs to probe ion reactivity, structure and stability

The Gas Phase, in the absence of solvent and counterions, allows to elucidate the **intrinsic behavior in ionic reactions** and expose the role of the environment.



APPLICATIONS

Thermodynamics
Kinetics
Reaction mechanisms

Organic chemistry
Organometallic catalysis
Functional group identification
Interstellar chemistry
Plasma chemistry

- Structure (isomer differentiation)
- Reactivity (intrinsic)
- Reaction Mechanisms
- Isolation and characterization of elusive intermediates



IMRs

Pros

- sensitivity
- specificity
- selectivity
- numerous reaction-based strategies
- no extensive purification/sample preparation
- (indirect) structural information

Cons

- inferred information on neutral products
- volatile neutrals (b.p. < 200 °C)

Gas phase ion molecule reactions

- **General aspects**
- **Instrumental details**
- **Bioinorganic studies @ Sapienza**



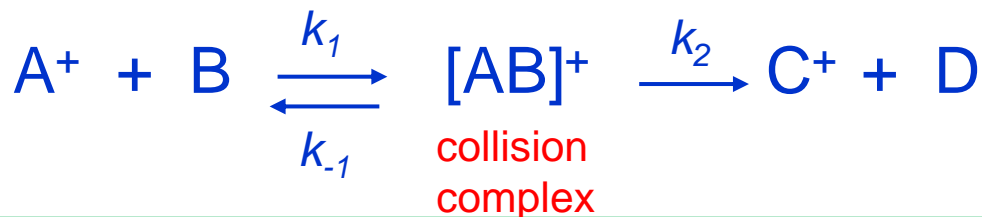
General aspects

Collision rate

number of charges in the ion

the greatest possible reaction rate

dipole moment and polarizability of the neutral



How to calculate the k_{coll}

Capture/collision rate : $k_{\text{coll}} \sim 1 \times 10^{-9} \text{ cm}^3 \text{ molecule}^{-1} \text{ s}^{-1}$

One or two order of magnitude larger than molecule-molecule reactions

ADO theory

ADO: averaged dipole orientation

$$k_{\text{ADO}} = \frac{2\pi q}{\sqrt{\mu}} \left\{ \sqrt{\alpha} + C\mu_{\text{D}} \left(\frac{2}{\pi k_{\text{B}} T} \right)^{1/2} \right\}$$

the first term is the Langevin contribution

μ is the reduced mass; μ_{D} is the permanent dipole;

C is a correction factor depending on $\mu_{\text{D}}/\alpha^{1/2}$;

k_{B} is Boltzmann's constant

kADO predicts accurately absolute proton transfer rate constants



Experimental rate constants



$$-\frac{dR(t)}{dt} = k n R(t) \quad \text{bimolecular reaction}$$

\uparrow
 $n = \text{number density of neutral N}$

In a conventional bimolecular process the number density of neutral reactant would decrease with time. Here, it does not.

$$I_{(t)} = I_0 e^{-nkt} \quad \text{pseudo-first order reaction}$$

$$\ln \frac{I_{(t)}}{I_0} = -nkt \quad k = k_{exp}$$



The total signal intensity is used to normalize the data and avoid errors from slight variations in the number of ions.

The signal intensity of $I_{(t)}$ can be monitored as a function of time and the rate constants for the disappearance of reactant ions and the appearance of product ions are obtained.



- The semilog plot of the decrease of the parent ion abundance with time is linearly interpolated and the **pseudo-first order rate constant** is obtained.
- The bimolecular rate constant (k_{exp}) at 300 K is gained from the ratio between the negative slope and n , the number density of the neutral.
- n is calculated from the ideal gas equation and allows to convert the measured value of the neutral pressure (mbar) in molecule cm^{-3} at 300 K.

$$k_{exp} = \frac{-\text{slope (s}^{-1}\text{)}}{n \text{ (molecule cm}^{-3}\text{)}} = \dots \text{ cm}^3 \text{ molecule}^{-1} \text{ s}^{-1}$$

Typically, the reproducibility of k_{exp} values is within 10%;
 while the error in the absolute rate constants is estimated to be $\pm 30\%$.
 It is mainly due to uncertainty in pressure measurements.



The efficiency (Φ) of an IMR can be determined by comparing the experimental rate constant (k_{exp}) with a theoretical estimate of the capture rate constant as percentages of the collision rate constant (k_{coll}).

$$\Phi = \frac{k_{exp}}{k_{coll}} \quad \text{measure of reaction probability per collision} \\ \text{(number of events that bring to reaction)}$$

Many exothermic reactions exhibit unit reaction probability at room T;
others proceed with reaction efficiency much less than unity.



Instrumental details

Where to perform IMR:

- Chemical ionization ion source
- Atmospheric pressure ion source
- rf-only quadrupole or a triple quadrupole
- Ion-trapping instruments: FT-ICR and linear quadrupole ion-trap (the most versatile MS)

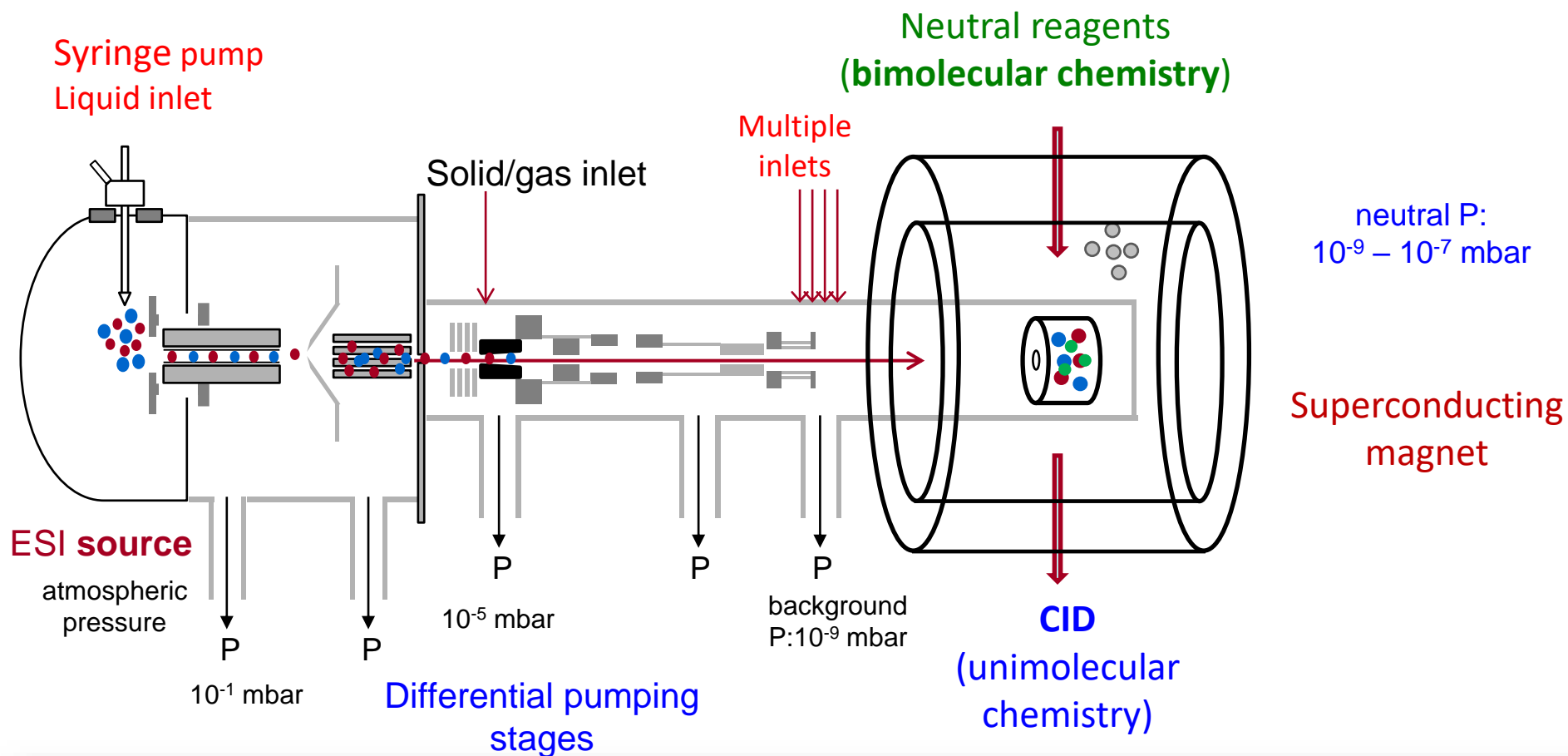
In FT-ICR:

- low pressure measurements (10^{-5} - 10^{-8} torr)
- reagent introduction with variable leak valves and/or pulsed valves
- time and energy control of reactions
- mass selection of reactant and product ions
- structural characterization by CID, ECD, IRMPD
- multistep MS^n sequences
- high resolution, high mass accuracy mode of operation



@Dipartimento di Chimica e Tecnologie del Farmaco, Roma

**Bruker Apex II,
4.7T FT-ICR MS**



Equipment for TNA in Roma



Types of Ion-Molecule Reactions

- Electron-Transfer
- Proton transfer
- H-atom/ O-atom transfer
- H/D exchange
- Functional-group selective
- Nucleophilic displacement
- Radiative association



Association Reactions

- solvation of an ion by weak electrostatic or hydrogen bonding;
- ion ligation involving bonds of intermediate strength;
- strong covalent bond formation



at the low operating pressures of the FT-ICR cell: thermal equilibration of the adduct ion via IR radiative emission

The rate of radiative emission is expected to increase with increasing size of the ion



Bioinorganic studies @ Sapienza

- search for site-specific addition reaction in heme-peptide/protein ions
- oxidation by cyt P450 model ions
- cation- π interactions



Functional-group selective IMR

J Biol Inorg Chem (2007) 12:22–35
DOI 10.1007/s00775-006-0159-9

ORIGINAL PAPER

**Heme-peptide/protein ions and phosphorous ligands:
search for site-specific addition reactions**

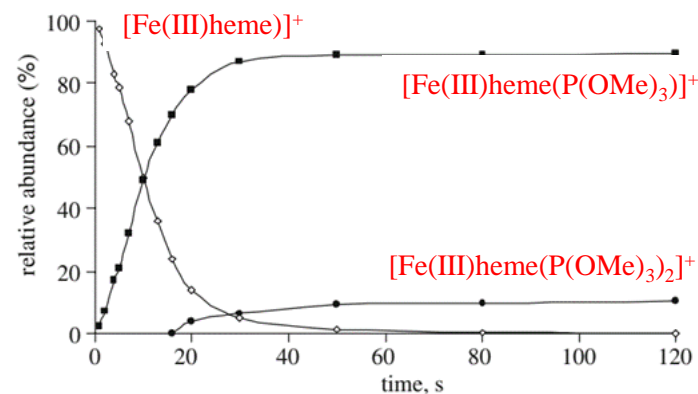
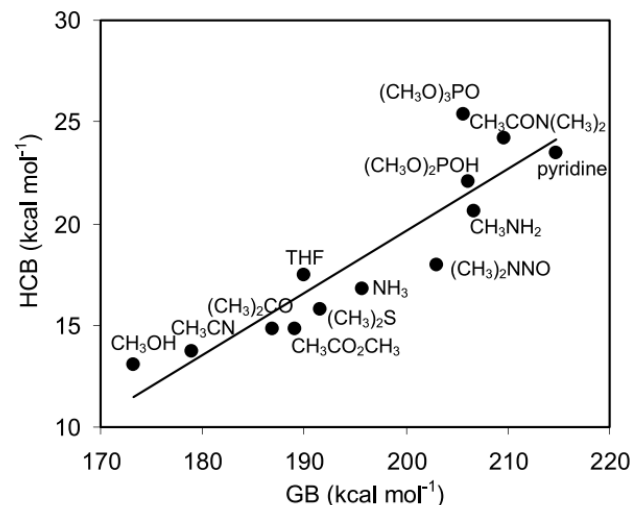
Maria Elisa Crestoni · Simonetta Fornarini

- Fe(III)-heme⁺
- MP11
- cyt c
- myoglobin

+ OP(OMe)₃ (GB: 206 kcal/mol)
+ P(OMe)₃ (GB: 215.3 kcal/mol)



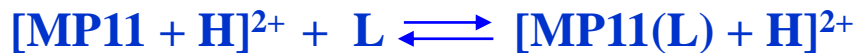
$$-\Delta G^\circ = RT \ln K = \frac{I(\text{Fe(III)-heme(L)})}{I(\text{Fe(III)heme}^+) \times P(\text{L})} = \text{HCB}(\text{L})$$



the back acceptor ability of P(OMe)₃ favors addition at the sixth coordination site



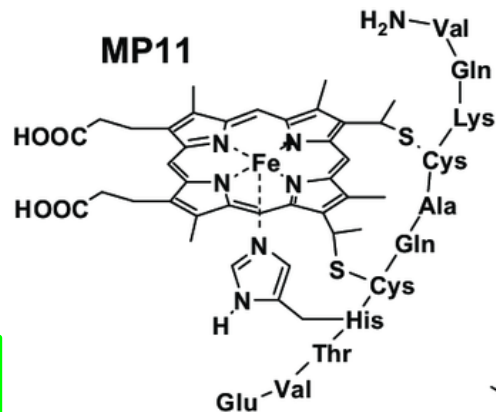
Functional-group selective IMR



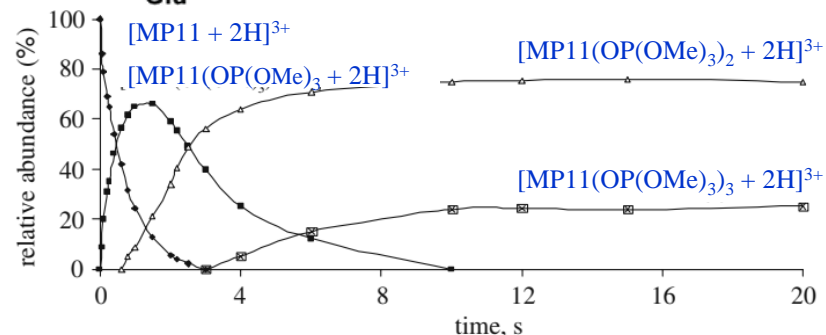
| | Φ | $-\Delta G^\circ$ (kcal mol ⁻¹) |
|--------------------------|--------|---|
| L = OP(OMe) ₃ | - | - |
| L = P(OMe) ₃ | 0.90 | 13.7 |



| | Φ | $-\Delta G^\circ$ (kcal mol ⁻¹) |
|--------------------------|--------|---|
| L = OP(OMe) ₃ | 10 | - |
| L = OP(OMe) ₃ | 2.6 | 14.4 (2 nd add.) |
| L = OP(OMe) ₃ | 0.80 | 12.8 (3 rd add.) |
| L = P(OMe) ₃ | 4.9 | - |



functional model
of peroxidase and
cyt P450



stepwise addition of three OP(OMe)₃ molecules

Role of conformational effects:

- folded conformation of +2 charge state;
- elongated conformation for the +3 charge state

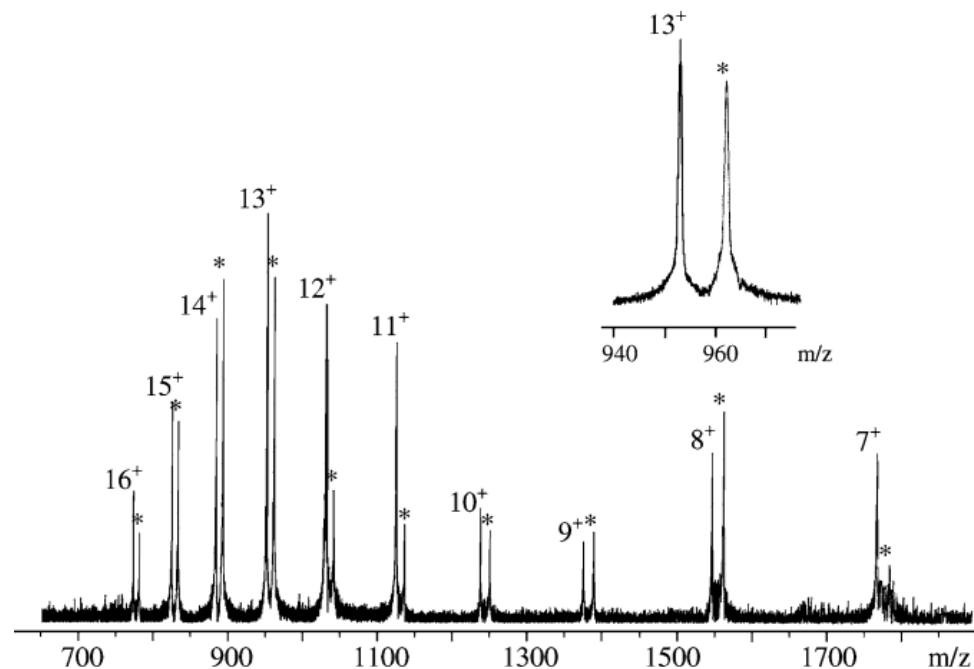
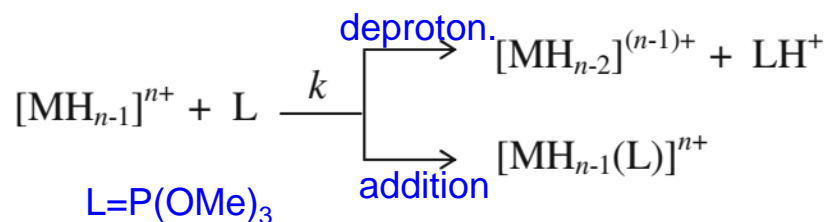
addition of one P(OMe)₃ molecule

Functional-group selective IMR

- multiply charged ions of cyt c

+ P(OMe)₃ (GB: 215.3 kcal/mol)

A cascade of competitive and sequential proton transfer and addition reactions occurs.



the addition reaction is limited to only one molecule of P(OMe)₃

The ΔG° values for the association of P(OMe)₃ with several multiply charged ions is the same as the one obtained with Fe(III)-heme(L)⁺ and [MP11+H]²⁺

The heme group with an axial ligand (the 5th) and a vacant site (the 6th) is a likely candidate of the association site in these multiply charged ions.

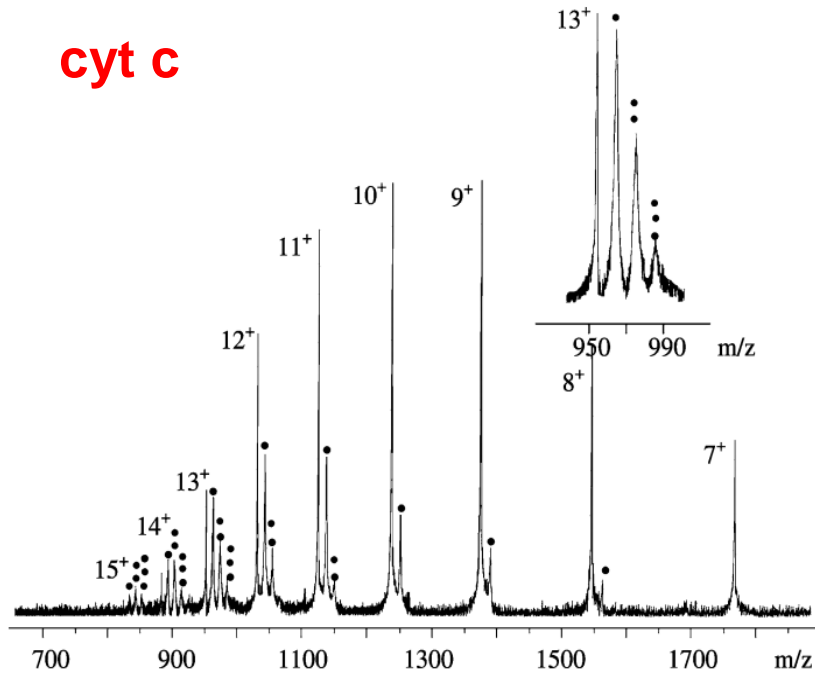


Functional-group selective IMR

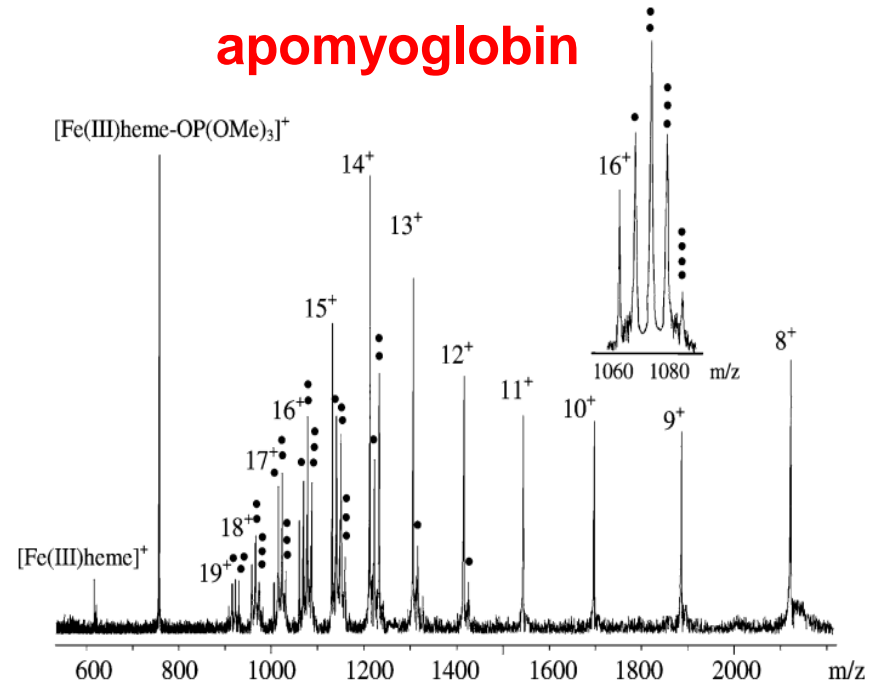
- multiply charged ions of cyt c
- multiply charged ions of apomyo

+ OP(OMe)₃ (GB: 206 kcal/mol)

cyt c



apomyoglobin



sequential addition of phosphate ligands due to the formation of proton-bound clusters



Functional-group selective IMR

- multiply charged ions of cyt c

+ OP(OMe)₃ / P(OMe)₃ (30:70)

the addition of phosphite is always limited to just one molecule, irrespective of charge state, in contrast with a charge-dependent number of added phosphate ligands

- OP(OMe)₃ is engaged in H bonding to protonated sites
- P(OMe)₃ is sampling the protein prosthetic group

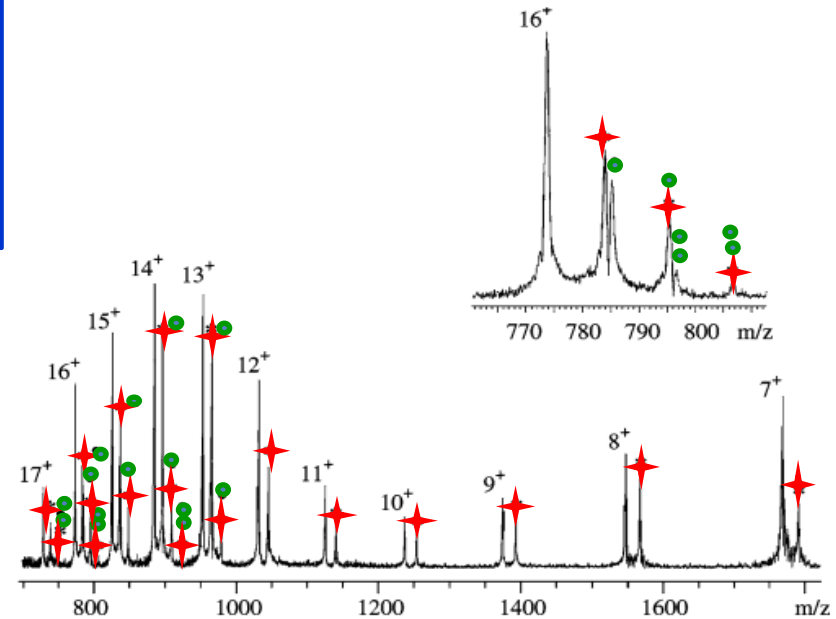


Fig. 9 FT-ICR mass spectrum of cyt *c* allowed to react with a 70:30 mixture of triethylphosphite, P(OEt)₃, and triethylphosphate, OP(OEt)₃, at 2.4×10^{-8} mbar for 3 s. Numbers denote the charge states of cyt *c* ions. Each charge state forms adducts with a single P(OEt)₃ molecule (represented by a star). The high charge states add up to four OP(OEt)₃ molecules; each OP(OMe)₃ molecule is represented by a circle

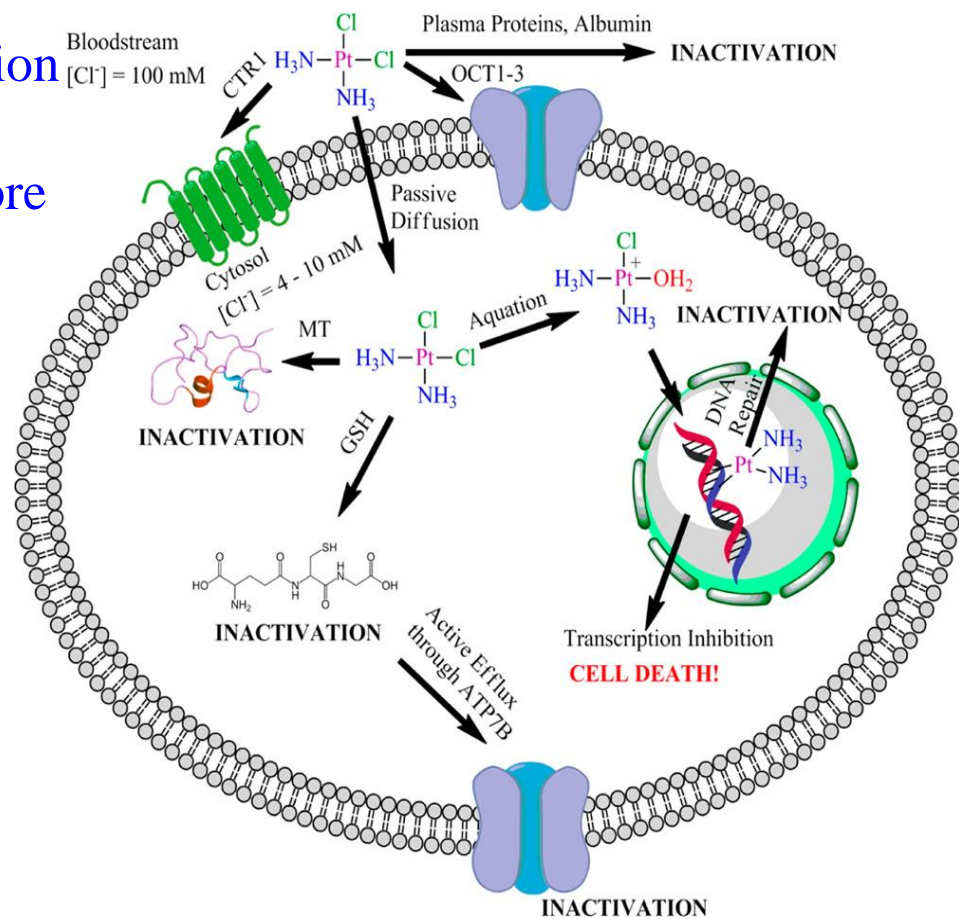
Hydrolysis of cis and transplatin

From ion-molecule reactions to the activation of non-covalent encounter complexes: mass spectrometry-based methods to explore the reactivity of metal complexes

Friday 16 December 2022 (10h45-11h30)

Young EU_FT-ICR_MS PI:

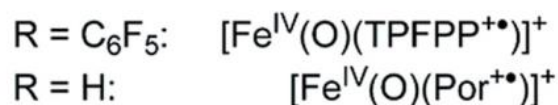
Daide Corinti (Roma, Italy)



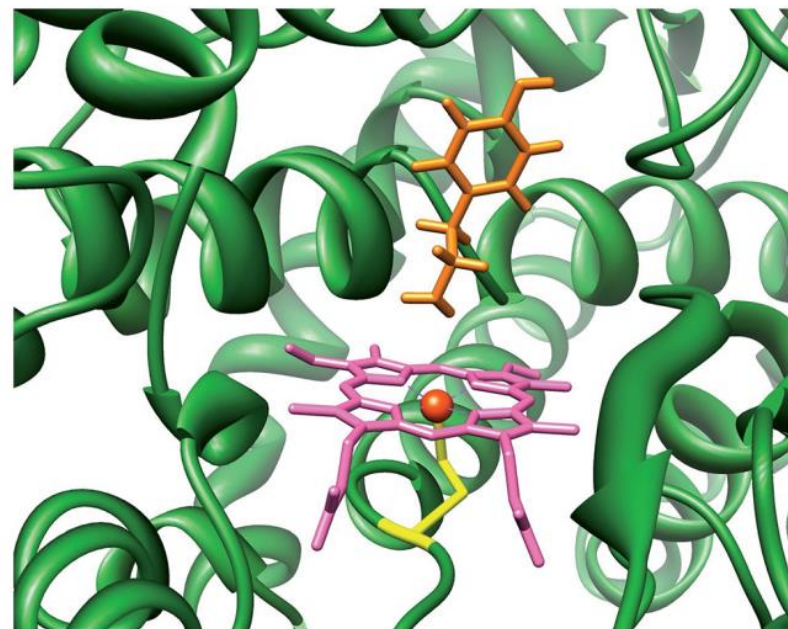
Biomimetic oxidation by iron(IV)-oxo porphyrin radical cation complexes



naked five-coordinate species



Oxygen Atom Transfer (OAT) to :
olefins
aliphatic hydrocarbons
aromatic hydrocarbons
amines
sulfites
phosphites



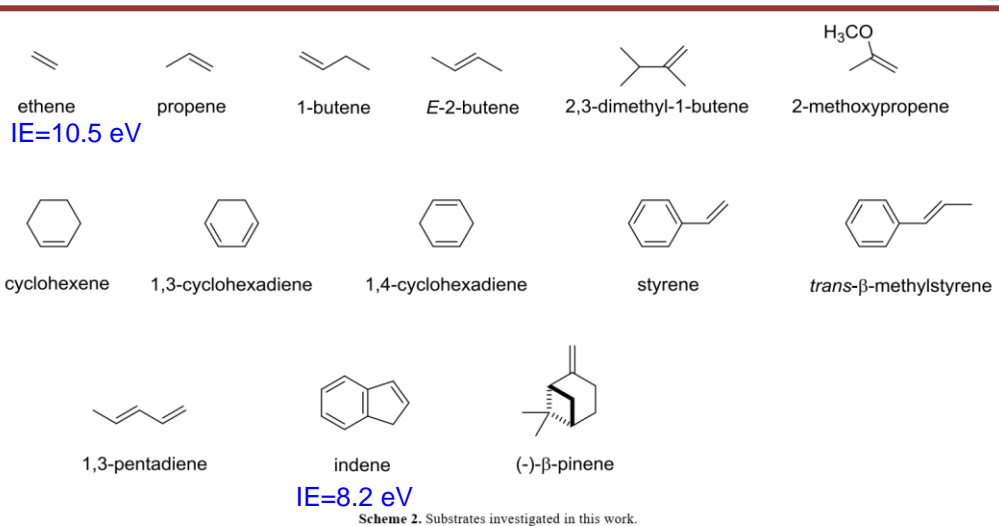
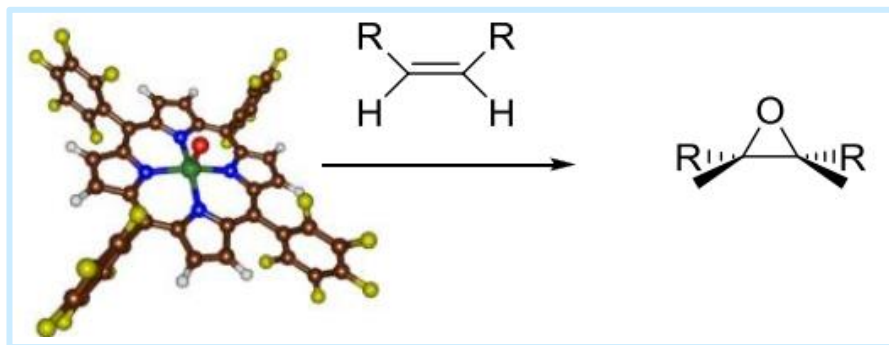
Active site of cyt P450. Substrate tyramine is in orange.



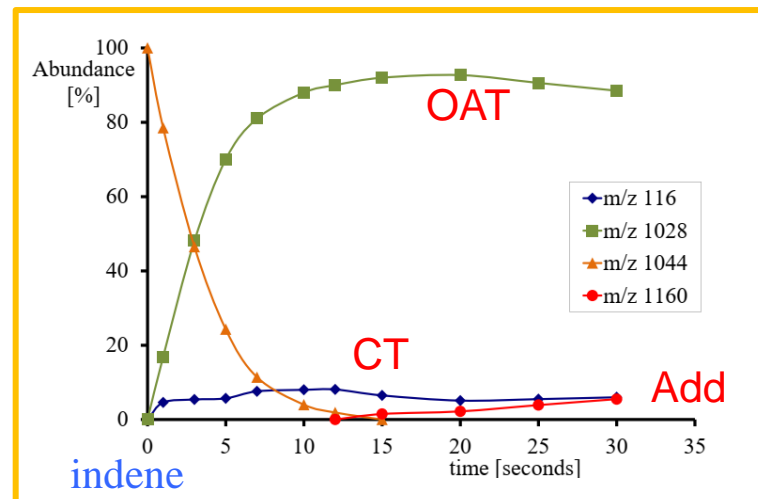
Cite this: Chem. Sci., 2015, 6, 1516

A comprehensive test set of epoxidation rate constants for iron(IV)-oxo porphyrin cation radical complexes†

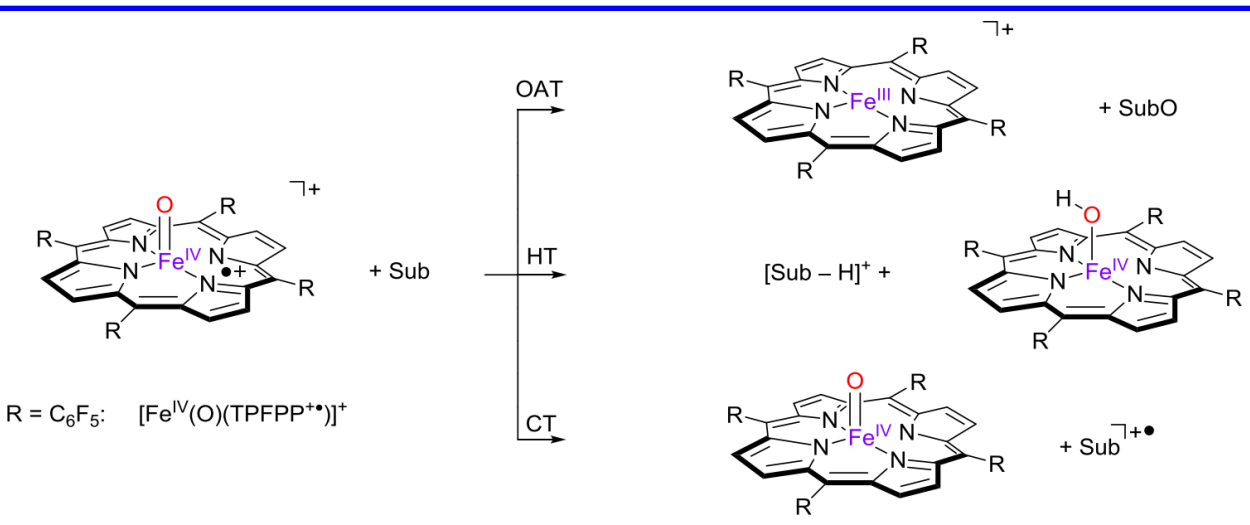
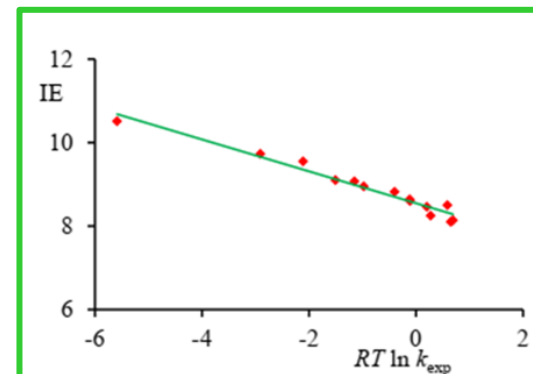
Mala A. Sainna,^a Suresh Kumar,^b Devesh Kumar,^{a,b} Simonetta Fornarini,^{a,c} Maria Elisa Crestoni^{a,c} and Sam P. de Visser^{a*}



Scheme 2. Substrates investigated in this work.



EA $[\text{Fe}^{\text{IV}}(\text{O})(\text{TPFP}^{\cdot+})]^+ < 8.2 \text{ eV}$



Reaction Mechanisms

A Systematic Account on Aromatic Hydroxylation by a Cytochrome P450 Model Compound I: A Low-Pressure Mass Spectrometry and Computational Study

Fabián G. Cantú Reinhard^{+, [a]} Mala A. Sainna^{+, [a]} Pranav Upadhyay^{, [b]} G. Alex Balan^{, [a]} Devesh Kumar^{, [b]} Simonetta Fornarini^{, * [c]} Maria Elisa Crestoni^{, * [c]} and Sam P. de Visser^{, * [a]}

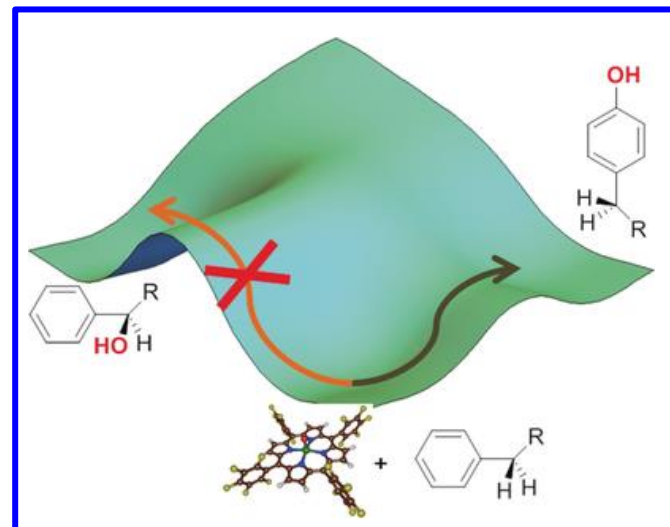
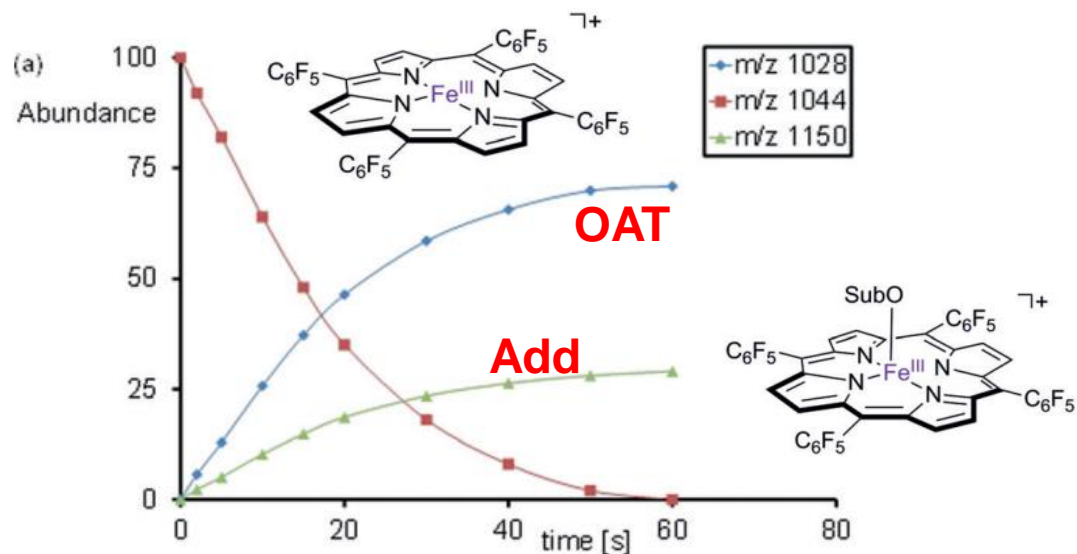


Table 1. FT-ICR MS reactivity of $[\text{Fe}^{\text{IV}}(\text{O})(\text{TPFPP}^+)]^+$ with arenes: Second-order rate constants, reaction efficiencies and product distributions for OAT and Add.

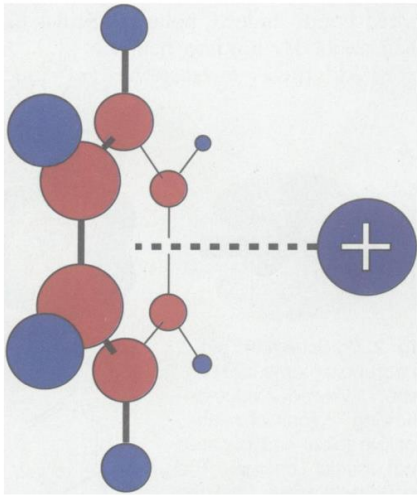
| Substrate | IE ^[a] | k_{exp} ^[b,c] | k_{ADO} ^[b] | Φ_{OAT} | Φ_{Add} | [%] OAT | [%] Add |
|--|-------------------|-----------------------------------|---------------------------------|---------------------|---------------------|---------|---------|
| benzaldehyde | 9.50 | 0.15 | 11.4 | – | 1.3 | 0 | 100 |
| α -[D ₁]-benzaldehyde | 9.50 | 0.14 | 11.4 | – | 1.2 | 0 | 100 |
| benzene | 9.20 | 0.012 | 8.8 | 0.14 | – | 100 | – |
| toluene | 8.80 | 0.36 | 9.2 | 3.1 | 0.78 | 80 | 20 |
| ethylbenzene | 8.77 | 0.58 | 9.5 | 4.3 | 1.8 | 70 | 30 |
| [D ₅]-ethylbenzene | 8.77 | 0.56 | 9.5 | 4.2 | 1.7 | 72 | 28 |
| [D ₁₀]-ethylbenzene | 8.77 | 0.57 | 9.5 | 4.4 | 1.6 | 73 | 27 |
| <i>i</i> -propylbenzene | 8.73 | 1.2 | 10.0 | 7.8 | 4.2 | 65 | 35 |
| <i>tert</i> -butylbenzene | 8.68 | 1.0 | 10.0 | 9.5 | 0.5 | 95 | 5 |
| <i>o</i> -xylene | 8.56 | 1.4 | 9.5 | 9.5 | 5.2 | 65 | 35 |
| [D ₄]- <i>o</i> -xylene | 8.56 | 1.4 | 9.5 | 9.1 | 5.6 | 62 | 38 |
| [D ₆]- <i>o</i> -xylene | 8.56 | 1.3 | 9.5 | 8.9 | 4.8 | 65 | 35 |
| <i>m</i> -xylene | 8.55 | 1.6 | 9.5 | 15.8 | 1.2 | 93 | 7 |
| <i>p</i> -xylene | 8.44 | 1.3 | 8.9 | 9.4 | 5.1 | 65 | 35 |
| mesitylene | 8.40 | 1.9 | 9.0 | 12.6 | 8.4 | 60 | 40 |
| naphthalene | 8.14 | 0.93 | 9.1 | 7.6 | 2.4 | 76 | 24 |



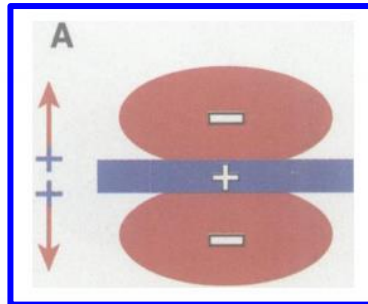
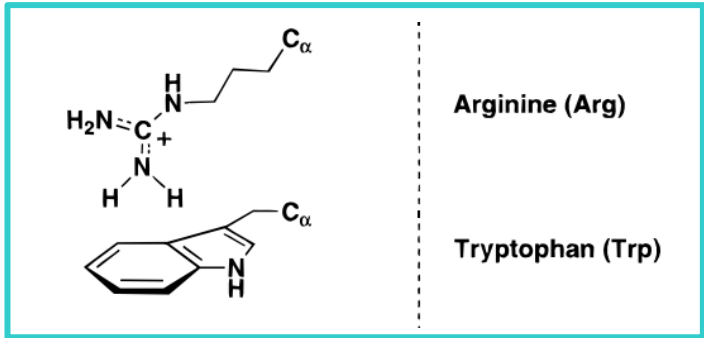
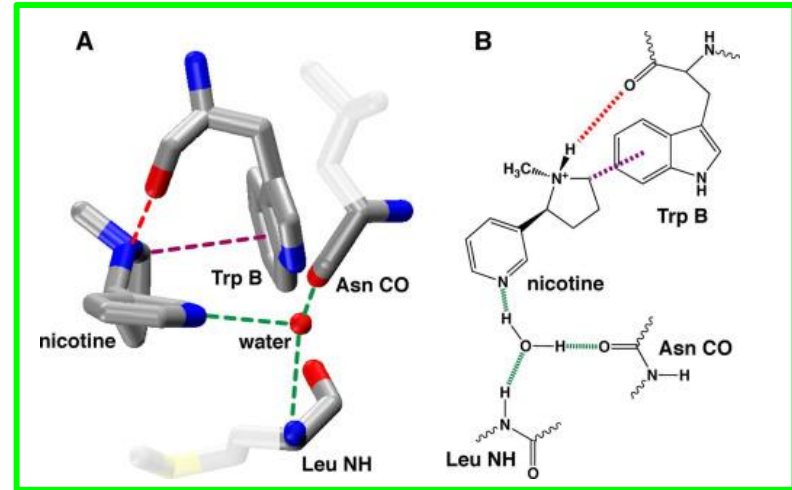
Dominant aromatic hydroxylation pathway and no evidence of aliphatic hydroxylation

Cation- π Interactions

- protein folding
- drug-receptor binding
- ion-transport through membranes

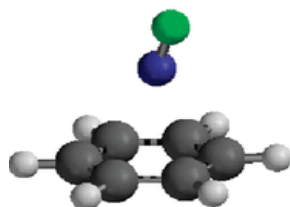


interaction dominated by electrostatic contact

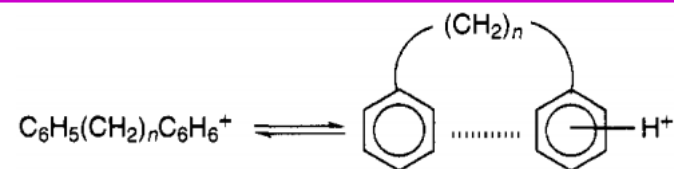


Schematic of the quadrupole moment of benzene

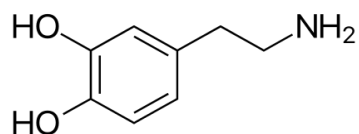
Gas-phase



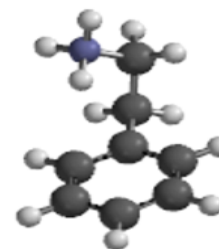
π -Complex Structure of Gaseous Benzene-NO Cations
Assayed by IR Multiple Photon Dissociation Spectroscopy
M. E. Crestoni et al., JACS 2006, 128, 12553-12561



Gas-Phase Protonation of α,ω -Diphenylalkanes
S. Fornarini et al.,
J. Phys. Chem. 1995, 99, 3150-3155



dopamine



Cation- π Interactions in Protonated Phenylalkylamines
S. Fornarini et al., JPCA 2014, 118, 7130-7138

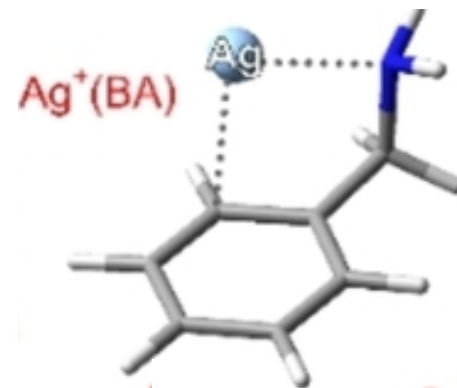
Cation- π Interactions between a Noble Metal and a Polyfunctional Aromatic Ligand: Ag^+ (benzylamine)

M. E. Crestoni et al., Chem. Eur. J. 2022, 28, e202200300

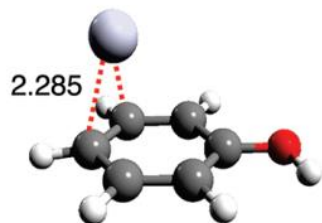
$\text{BE}(\text{Ag}^+\text{-benzene}) = 38 \text{ kcal/mol}$

$\text{IE}(\text{Ag}) = 7.58 \text{ eV}$

$\text{IE}(\text{benzene}) = 9.24 \text{ eV}$



$\text{BE}_{\text{ring}} = 41.6 \text{ kcal/mol}$



$\text{BE}_{\text{OH}} = 31.3 \text{ kcal/mol}$

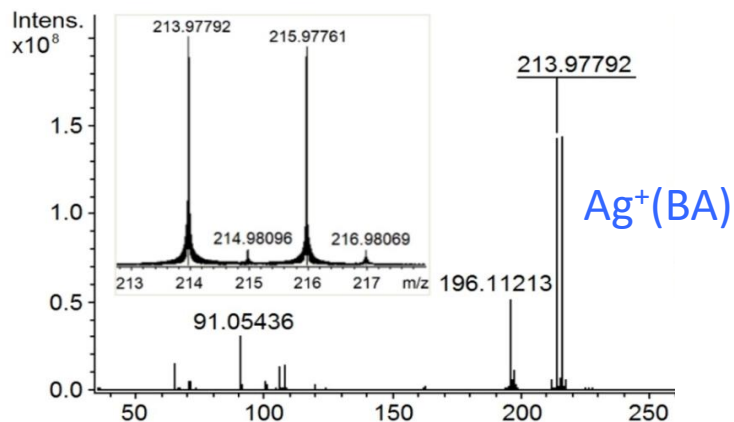
Structure and Infrared Spectrum of the Ag^+ -Phenol Ionic Complex

O. Dopfer et al., J.Phys Chem A 2010, 114, 11053-11059

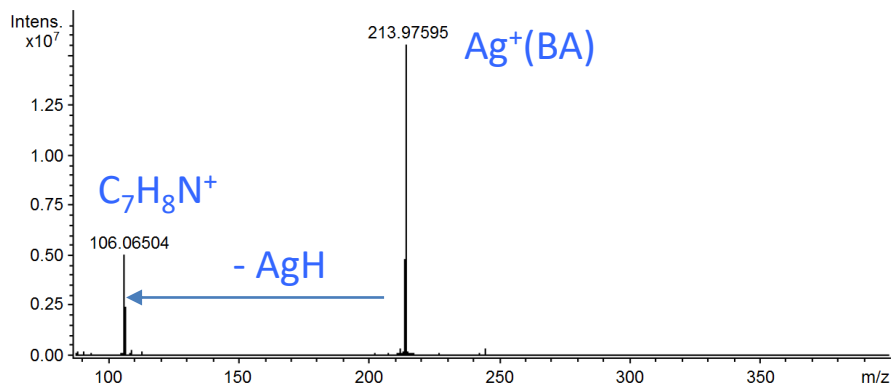
establish the role of cation-N and cation- π interactions
in the Ag^+ (benzylamine) complex



CID experiments

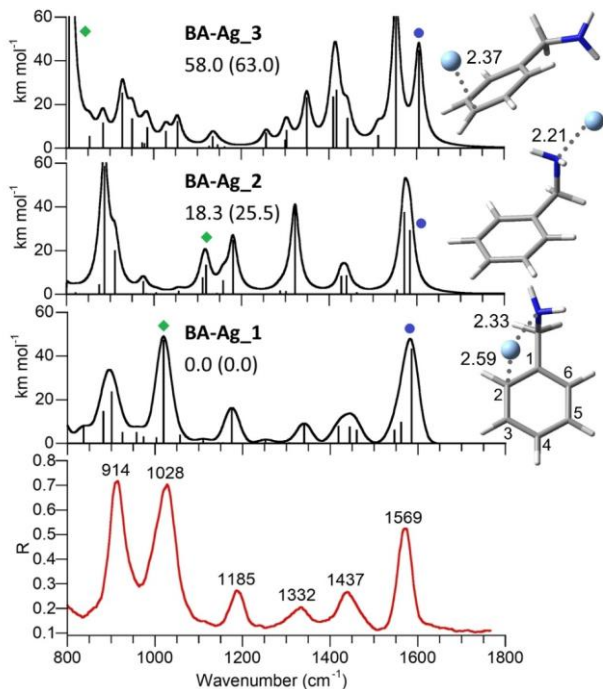


ESI FT-ICR mass spectrum of a (1:1) μM solution of BA and AgNO_3



Collision induced dissociation experiment conducted on $\text{Ag}^+(\text{BA})$ ions (m/z 214)

IRMPD spectroscopy @ CLIO



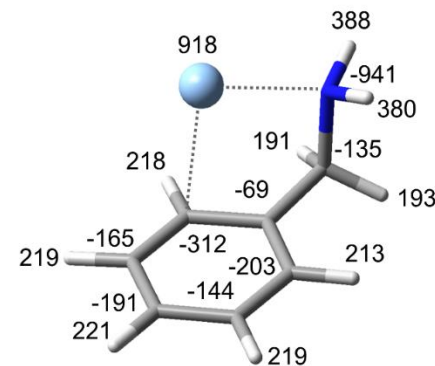
$\text{Ag}^+ - \pi$

$\text{N} - \text{Ag}^+$

$\text{N} - \text{Ag}^+ - \pi$

$\text{BE}(\text{Ag}^+ - \text{BA}) = 55.7 \text{ kcal/mol}$

- sciss NH_2 @ 1585 cm^{-1} in **BA-Ag_1** and **BA-Ag_2**
@ 1605 cm^{-1} in **BA-Ag_3**
- wag NH_2 @ 1020 cm^{-1} in **BA-Ag_1**
@ 1129 cm^{-1} in **BA-Ag_2**
@ 807 cm^{-1} in **BA-Ag_3**

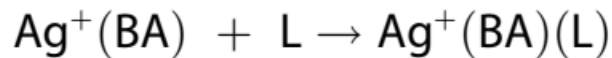


NBO charge distribution (in me)

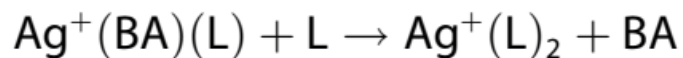
$\text{IE}(\text{Ag}) = 7.58 \text{ eV}$

$\text{IE}(\text{BA}) = 8.5 \text{ eV}$

Ion-molecule reactions



L = toluene, mesitylene, pyridine, piperidine



L = piperidine

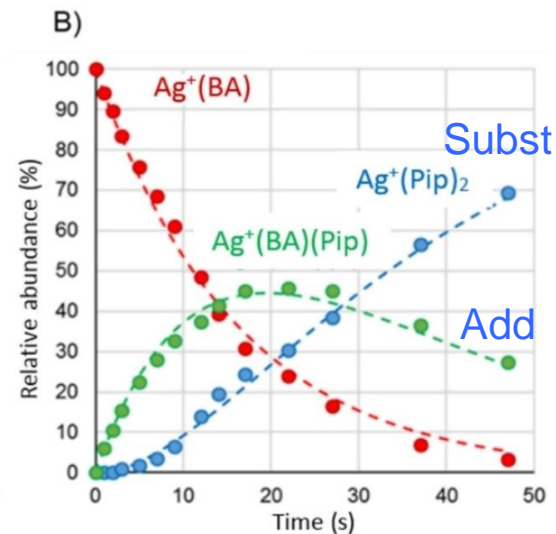
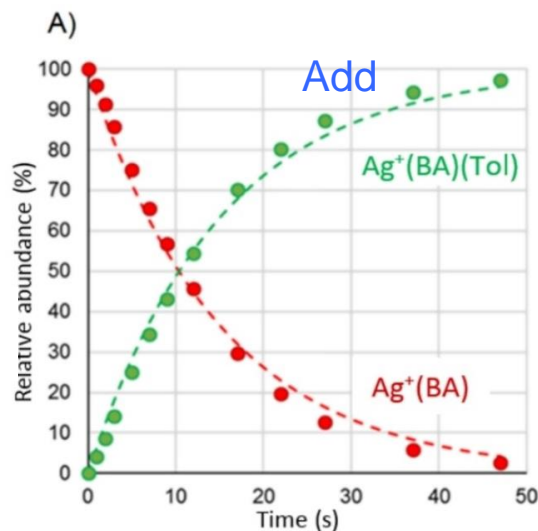


Table 2. Kinetic data for the gas phase reaction of $\text{Ag}^+(\text{BA})$ ions with selected neutrals (L).

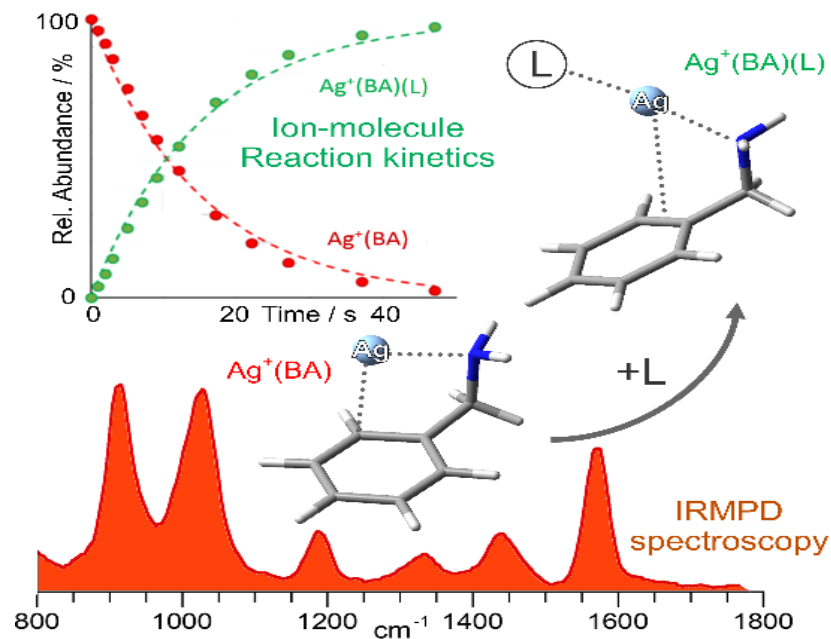
| L | Proton affinity [kJ mol ⁻¹] ^[68] | Na ⁺ -BE (kJ/mol) | k_{exp} [10 ⁻¹⁰ cm ³ molecule ⁻¹ s ⁻¹] | Φ ^[a] |
|---------------------------|--|---------------------------------|---|-----------------------|
| Toluene | 784 | 113 | 1.2 | 12 |
| Mesitylene | 836 | - | 3.4 | 31 |
| Pyridine | 930 | 127 | 3.7 | 24 |
| Piperidine ^[b] | 954 | - | 5.8 | 47 |

[a] Reaction efficiency: $\Phi = (k_{\text{exp}}/k_{\text{coll}}) \times 100$. [b] A rate constant $k_2 = 0.34 \times 10^{-10}$ cm³ molecule⁻¹ s⁻¹ is obtained for the ligand displacement [Equation (2)].^[62]

BA

913





- the increased silver coordination in $\text{Ag}^+(\text{BA})(\text{L})$ yields folded structures
- the affinity of π -ligands is quite comparable to that of N-ligands
- remarkable affinity of Ag^+ for π -donors

Dip. CTF

Simonetta Fornarini

Barbara Chiavarino

Davide Corinti

Alessandro Maccelli

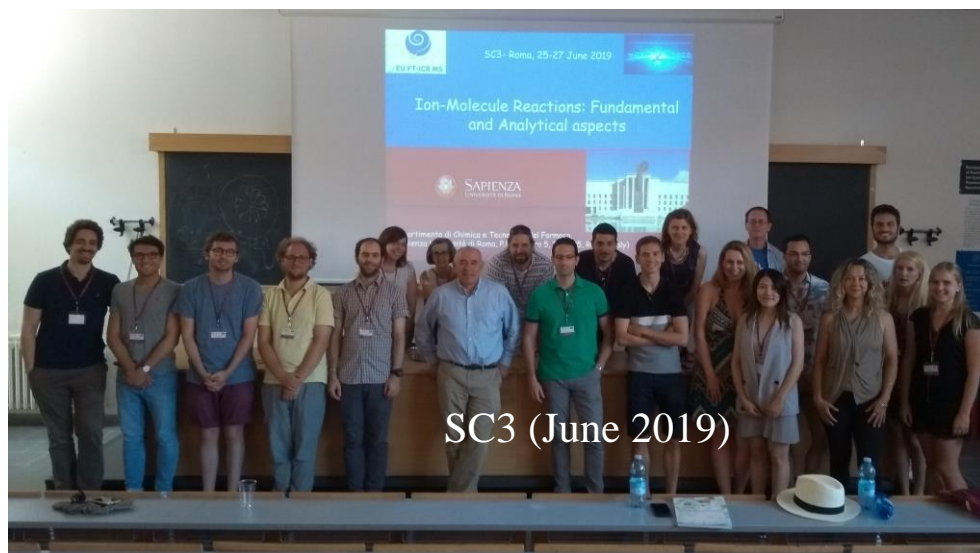
Alba Lasalvia

Lucretia Rotari

Valentina Lilla



SAPIENZA
UNIVERSITÀ DI ROMA



Thank you for the kind attention



SAPIENZA
UNIVERSITÀ DI ROMA

EUS2- Lille, 12-16 December 2022



SAPIENZA
UNIVERSITÀ DI ROMA



Greetings from SAPIENZA

